Supplementary Materials

Influence of the Computer-aided Decision Support System Design on Ultrasound-Based Breast Cancer Classification

Supplementary Information

Table S1. The precision metrics (recall, precision, and F1-Score) calculated with reference to the IoU score for the best YOLOv3 detection models, trained with transfer learning by "fine tuning" and "freezing layers", applied on the validation set.

Dataset	Method	IoU (mean + STD)	Recall	Precision	F1-Score
D1: All Augmentations	"fine tuning"	0.5108 ± 0.0633	0.708	0.913	0.797
	"freezing layers"	0.4839 ± 0.0528	0.741	0.818	0.778
D2: UDWT + Spatial	"fine tuning"	0.5163 ± 0.0628	0.756	0.932	0.834
	"freezing layers"	0.3372 ± 0.0435	0.525	0.667	0.587
D3: EXP + Spatial	"fine tuning"	0.5087 ± 0.0596	0.753	0.905	0.822
	"freezing layers"	0.3383 ± 0.0429	0.536	0.804	0.643
D4: LN + Spatial	"fine tuning"	0.5362 ± 0.0640	0.824	0.805	0.814
	"freezing layers"	0.3929 ± 0.0485	0.567	0.895	0.694
D5: LoG + Spatial	"fine tuning"	0.5362 ± 0.0640	0.824	0.805	0.814
	"freezing layers"	0.3529 ± 0.0488	0.561	0.742	0.639
D6: Spatial Only	"fine tuning"	0.5085 ± 0.0647	0.688	0.970	0.805
	"freezing layers"	0.4123 ± 0.0503	0.632	0.797	0.705
D7: SQRT + Spatial	"fine tuning"	0.5403 ± 0.0722	0.773	0.883	0.824
	"freezing layers"	0.3489 ± 0.0468	0.554	0.730	0.630
D8: SQUARED + Spatial	"fine tuning"	0.5127 ± 0.0609	0.779	0.838	0.807
	"freezing layers"	0.3595 ± 0.0468	0.529	0.821	0.643

Abbreviations: UDWT, Undecimated Discrete Wavelet Transform; EXP, exponential; LN, logarithm; LoG, Laplacian of Gaussian; SQRT, square root; SQUARED, squared.

Table S2. The precision metrics (recall, precision, and F1-Score) calculated with reference to the LE score for the best YOLOv3 detection models, trained with transfer learning by 'fine tuning' and 'freezing layers', applied on the validation set.

Dataset	Method	LE (mean + STD)	Recall	Precision	F1-Score
D1: All Augmentations	"fine tuning"	0.2803 ± 0.0035	0.723	0.986	0.834
	"freezing layers"	0.2662 ± 0.0067	0.750	0.857	0.800
D2: UDWT + Spatial	"fine tuning"	0.2470 ± 0.0048	0.761	0.959	0.848
	"freezing layers"	0.4236 ± 0.0071	0.573	0.810	0.671
D3: EXP + Spatial	"fine tuning"	0.2499 ± 0.0051	0.763	0.959	0.850
	"freezing layers"	0.4369 ± 0.0058	0.557	0.875	0.681
D4: LN + Spatial	"fine tuning"	0.1823 ± 0.0058	0.835	0.874	0.854
	"freezing layers"	0.4222 ± 0.0042	0.576	0.930	0.711
D5: LoG + Spatial	"fine tuning"	0.1823 ± 0.0058	0.835	0.874	0.854
	"freezing layers"	0.4111 ± 0.0090	0.586	0.823	0.685
D6: Spatial Only	"fine tuning"	0.3122 ± 0.0044	0.691	0.985	0.813
	"freezing layers"	0.3514 ± 0.0071	0.648	0.855	0.738
D7: SQRT + Spatial	"fine tuning"	0.2273 ± 0.0063	0.783	0.935	0.852
	"freezing layers"	0.4054 ± 0.0057	0.589	0.841	0.693
D8: SQUARED + Spatial	"fine tuning"	0.2195 ± 0.0074	0.789	0.888	0.835
	"freezing layers"	0.4402 ± 0.0036	0.554	0.911	0.689

Abbreviations: UDWT, Undecimated Discrete Wavelet Transform; EXP, exponential; LN, logarithm; LoG, Laplacian of Gaussian; SQRT, square root; SQUARED, squared.

Table S3. The precision metrics (recall, precision, and F1-Score) calculated with reference to the IoU score for the best YOLOv3 and Viola-Jones detection models applied on the validation set. The metrics for the outstanding detection methods were underlined and bolded.

Dataset	Method	IoU (mean + STD)	Recall	Precision	F1-Score
D1: All Augmentations	Viola-Jones	0.4454 ± 0.0553	0.911	0.567	0.699
	YOLOv3	0.5108 ± 0.0633	0.708	0.913	0.797
D2: UDWT + Spatial	Viola-Jones	0.4179 ± 0.0491	0.842	0.558	0.671
	YOLOv3	0.5163 ± 0.0628	0.756	0.932	0.834
D3: EXP + Spatial	**Viola-Jones**	**0.3992 ± 0.0544**	**0.958**	**0.495**	**0.652**
	YOLOv3	0.5087 ± 0.0596	0.753	0.905	0.822
D4: LN + Spatial	Viola-Jones	0.4208 ± 0.0571	0.943	0.543	0.690
	YOLOv3	**0.5362 ± 0.0640**	**0.824**	**0.805**	**0.814**
D5: LoG + Spatial	Viola-Jones	0.3677 ± 0.0493	0.849	0.517	0.643
	YOLOv3	0.5362 ± 0.0640	0.824	0.805	0.814
D6: Spatial Only	Viola-Jones	0.4066 ± 0.0519	0.939	0.500	0.652
	YOLOv3	0.5085 ± 0.0647	0.688	0.970	0.805
D7: SQRT + Spatial	Viola-Jones	0.3801 ± 0.0497	0.797	0.566	0.662
	YOLOv3	0.5403 ± 0.0722	0.773	0.883	0.824
D8: SQUARED + Spatial	Viola-Jones	0.3990 ± 0.052	0.922	0.516	0.662
	YOLOv3	0.5127 ± 0.0609	0.779	0.838	0.807

Abbreviations: UDWT, Undecimated Discrete Wavelet Transform; EXP, exponential; LN, logarithm; LoG, Laplacian of Gaussian; SQRT, square root; SQUARED, squared.

Table S4. The precision metrics (recall, precision, and F1-Score) calculated with reference to the LE score for the best YOLOv3 and Viola-Jones detection models applied on the validation set. The metrics for the outstanding detection methods were underlined and bolded.

Dataset	Method	LE (mean + STD)	Recall	Precision	F1-Score
D1: All Augmentations	Viola-Jones	0.1389 ± 0.0132	0.932	0.767	0.841
	YOLOv3	0.2803 ± 0.0035	0.723	0.986	0.834
D2: UDWT + Spatial	Viola-Jones	0.1779 ± 0.0120	0.880	0.767	0.820
	YOLOv3	0.2470 ± 0.0048	0.761	0.959	0.848
D3: EXP + Spatial	**Viola-Jones**	**0.1208 ± 0.0146**	**0.970**	**0.699**	**0.813**
	YOLOv3	0.2499 ± 0.0051	0.763	0.959	0.850
D4: LN + Spatial	Viola-Jones	0.1144 ± 0.0139	0.957	0.728	0.827
	YOLOv3	**0.1823 ± 0.0058**	**0.835**	**0.874**	**0.854**
D5: LoG + Spatial	Viola-Jones	0.1886 ± 0.0127	0.882	0.690	0.774
	YOLOv3	0.1823 ± 0.0058	0.835	0.874	0.854
D6: Spatial Only	Viola-Jones	0.1236 ± 0.0126	0.958	0.739	0.834
	YOLOv3	0.3122 ± 0.0044	0.691	0.985	0.813
D7: SQRT + Spatial	Viola-Jones	0.1532 ± 0.0137	0.833	0.723	0.774
	YOLOv3	0.2273 ± 0.0063	0.783	0.935	0.852
D8: SQUARED + Spatial	Viola-Jones	0.1369 ± 0.0142	0.942	0.714	0.813
	YOLOv3	0.2195 ± 0.0074	0.789	0.888	0.835

Abbreviations: UDWT, Undecimated Discrete Wavelet Transform; EXP, exponential; LN, logarithm; LoG, Laplacian of Gaussian; SQRT, square root; SQUARED, squared.

Table S5. The precision metrics (recall, precision, and F1-Score) calculated with reference to the IoU score for the best YOLOv3 and Viola-Jones detection models applied on **the test set**. The metrics for the outstanding detection methods were underlined and bolded.

Dataset	Method	IoU (mean + STD)	Recall	Precision	F1-Score
D1: All Augmentations	**Viola-Jones**	**0.3986 ± 0.0540**	**0.959**	**0.500**	**0.657**
	YOLOv3	0.4390 ± 0.0636	0.626	0.919	0.745
D2: UDWT + Spatial	Viola-Jones	0.3906 ± 0.0458	0.868	0.517	0.648
	YOLOv3	0.5044 ± 0.0638	0.733	0.917	0.815
D3: EXP + Spatial	Viola-Jones	0.3426 ± 0.0477	0.944	0.362	0.523
	YOLOv3	0.3998 ± 0.0569	0.612	0.788	0.689
D4: LN + Spatial	Viola-Jones	0.3555 ± 0.0486	0.902	0.402	0.556
	YOLOv3	**0.5442 ± 0.0808**	**0.835**	**0.759**	**0.795**
D5: LoG + Spatial	Viola-Jones	0.3687 ± 0.0465	0.872	0.456	0.599
	YOLOv3	0.5329 ± 0.0785	0.823	0.756	0.788
D6: Spatial Only	Viola-Jones	0.3795 ± 0.0542	0.860	0.483	0.619
	YOLOv3	0.5003 ± 0.0586	0.696	0.914	0.790
D7: SQRT + Spatial	Viola-Jones	0.3602 ± 0.0461	0.843	0.489	0.619
	YOLOv3	0.4862 ± 0.0710	0.713	0.873	0.785
D8: SQUARED + Spatial	Viola-Jones	0.3447 ± 0.0461	0.854	0.389	0.534
	YOLOv3	0.5152 ± 0.0640	0.805	0.833	0.819

Abbreviations: UDWT, Undecimated Discrete Wavelet Transform; EXP, exponential; LN, logarithm; LoG, Laplacian of Gaussian; SQRT, square root; SQUARED, squared.

Table S6. The precision metrics (recall, precision, and F1-Score) calculated with reference to the LE score for the best YOLOv3 and Viola-Jones detection models applied on **the test set**. The metrics for the outstanding detection methods were underlined and bolded.

Dataset	Method	LE (mean + STD)	Recall	Precision	F1-Score
D1: All Augmentations	**Viola-Jones**	**0.0959 ± 0.0162**	**0.972**	**0.734**	**0.836**
	YOLOv3	0.3741 ± 0.0071	0.630	0.935	0.753
D2: UDWT + Spatial	Viola-Jones	0.1560 ± 0.0126	0.908	0.775	0.836
	YOLOv3	0.2698 ± 0.0047	0.739	0.944	0.829
D3: EXP + Spatial	Viola-Jones	0.1066 ± 0.0151	0.969	0.660	0.785
	YOLOv3	0.3667 ± 0.0086	0.637	0.879	0.739
D4: LN + Spatial	Viola-Jones	0.1205 ± 0.0145	0.944	0.739	0.829
	YOLOv3	**0.1706 ± 0.0094**	**0.856**	**0.885**	**0.830**
D5: LoG + Spatial	Viola-Jones	0.1420 ± 0.0153	0.915	0.722	0.807
	YOLOv3	0.1801 ± 0.0090	0.844	0.884	0.864
D6: Spatial Only	Viola-Jones	0.1385 ± 0.0134	0.907	0.764	0.829
	YOLOv3	0.3020 ± 0.0048	0.702	0.943	0.805
D7: SQRT + Spatial	Viola-Jones	0.1533 ± 0.0136	0.889	0.727	0.800
	YOLOv3	0.2815 ± 0.0079	0.725	0.930	0.815
D8: SQUARED + Spatial	Viola-Jones	0.1430 ± 0.0150	0.913	0.700	0.792
	YOLOv3	0.2088 ± 0.0094	0.811	0.869	0.839

Abbreviations: UDWT, Undecimated Discrete Wavelet Transform; EXP, exponential; LN, logarithm; LoG, Laplacian of Gaussian; SQRT, square root; SQUARED, squared.

Table S7. The precision metrics (recall, precision, and F1-Score) calculated with reference to the IoU score for the best YOLOv3 and Viola-Jones detection models applied on the second data pool. The metrics for the outstanding detection methods were underlined and bolded.

Dataset	Method	IoU (mean + STD)	Recall	Precision	F1-Score
D1: All Augmentations	Viola-Jones	0.2825 ± 0.0512	0.817	0.331	0.471
	YOLOv3	0.3485 ± 0.0512	0.540	0.753	0.629
D2: UDWT + Spatial	Viola-Jones	0.2631± 0.0470	0.802	0.316	0.454
	YOLOv3	0.3819 ± 0.0594	0.609	0.729	0.664
D3: EXP + Spatial	Viola-Jones	0.2443 ± 0.0493	0.873	0.232	0.367
	YOLOv3	0.3520 ± 0.0511	0.547	0.792	0.647
D4: LN + Spatial	**Viola-Jones**	**0.2654 ± 0.0560**	**0.896**	**0.257**	**0.400**
	YOLOv3	**0.4247 ± 0.0609**	**0.729**	**0.664**	**0.695**
D5: LoG + Spatial	Viola-Jones	0.2681 ± 0.0565	0.855	0.269	0.409
	YOLOv3	0.4247 ± 0.0609	0.729	0.664	0.695
D6: Spatial Only	Viola-Jones	0.2886 ± 0.0545	0.845	0.335	0.479
	YOLOv3	0.3241 ± 0.0436	0.479	0.758	0.587
D7: SQRT + Spatial	Viola-Jones	0.2753 ± 0.0526	0.806	0.341	0.479
	YOLOv3	0.3885 ± 0.0595	0.591	0.761	0.665
D8: SQUARED + Spatial	Viola-Jones	0.2807 ± 0.0553	0.854	0.313	0.458
	YOLOv3	0.4273 ± 0.0689	0.723	0.719	0.721

Abbreviations: UDWT, Undecimated Discrete Wavelet Transform; EXP, exponential; LN, logarithm; LoG, Laplacian of Gaussian; SQRT, square root; SQUARED, squared.

Table S8. The precision metrics (recall, precision, and F1-Score) calculated with reference to the LE score for the best YOLOv3 and Viola-Jones detection models applied on the second data pool. The metrics for the outstanding detection methods were underlined and bolded.

Dataset	Method	LE (mean + STD)	Recall	Precision	F1-Score
D1: All Augmentations	Viola-Jones	0.2428 ± 0.0392	0.886	0.572	0.695
	YOLOv3	0.4125 ± 0.0085	0.584	0.900	0.708
D2: UDWT + Spatial	Viola-Jones	0.2736 ± 0.0396	0.869	0.520	0.650
	YOLOv3	0.3471 ± 0.0116	0.656	0.896	0.758
D3: EXP + Spatial	Viola-Jones	0.2426 ± 0.0384	0.934	0.479	0.634
	YOLOv3	0.4181 ± 0.0083	0.583	0.917	0.713
D4: LN + Spatial	**Viola-Jones**	**0.2187 ± 0.0378**	**0.948**	**0.549**	**0.695**
	YOLOv3	**0.2491 ± 0.0168**	**0.769**	**0.821**	**0.794**
D5: LoG + Spatial	Viola-Jones	0.2310 ± 0.0387	0.917	0.504	0.650
	YOLOv3	0.2491 ± 0.0168	0.769	0.821	0.794
D6: Spatial Only	Viola-Jones	0.2285 ± 0.0376	0.901	0.562	0.692
	YOLOv3	0.4760 ± 0.0085	0.512	0.863	0.642
D7: SQRT + Spatial	Viola-Jones	0.2628 ± 0.0363	0.873	0.565	0.686
	YOLOv3	0.3635 ± 0.0090	0.641	0.940	0.762
D8: SQUARED + Spatial	Viola-Jones	0.2326 ± 0.0366	0.912	0.553	0.689
	YOLOv3	0.2565 ± 0.0151	0.760	0.873	0.813

Abbreviations: UDWT, Undecimated Discrete Wavelet Transform; EXP, exponential; LN, logarithm; LoG, Laplacian of Gaussian; SQRT, square root; SQUARED, squared.

Table S9. Radiomics features identified in the analysis of the Manual Segmentation dataset and their lambda score.

Feature Name	Lambda
original_glcm_Imc2	0.011928
original_glszm_LowGrayLevelZoneEmphasis	0.023903
exponential_glcm_Imc1	0.007132
exponential_glrlm_GrayLevelNonUniformity	0.037015
exponential_glrlm_HighGrayLevelRunEmphasis	-0.01403
exponential_glrlm_RunEntropy	0.048686
exponential_glszm_SmallAreaLowGrayLevelEmphasis	0.004808
gradient_firstorder_Skewness	-0.09664
gradient_glrlm_RunEntropy	0.130352
gradient_glrlm_ShortRunLowGrayLevelEmphasis	-0.06101
logarithm_glcm_Contrast	-0.03666
logarithm_glcm_Idmn	0.020441
logarithm_glcm_Imc2	0.019052
logarithm_glrlm_RunVariance	-0.023
logarithm_glszm_GrayLevelNonUniformityNormalized	-0.04194
squareroot_glrlm_LongRunHighGrayLevelEmphasis	-0.01728
squareroot_glszm_LargeAreaHighGrayLevelEmphasis	-0.01028
squareroot_glszm_SmallAreaHighGrayLevelEmphasis	-0.00084
wavelet-LH_firstorder_Mean	-0.01353
wavelet-LH_firstorder_Skewness	-0.04576
wavelet-LH_glcm_Imc1	0.026884
wavelet-LH_glszm_SmallAreaEmphasis	-0.11354
wavelet-LH_ngtdm_Contrast	0.012435
wavelet-HL_firstorder_Energy	0.020368
wavelet-HL_firstorder_TotalEnergy	1.28E-17
wavelet-HL_glrlm_GrayLevelNonUniformityNormalized	-0.02213
wavelet-HL_glrlm_ShortRunEmphasis	0.081554
wavelet-HL_glszm_SmallAreaEmphasis	0.036429
wavelet-HH_glszm_GrayLevelVariance	0.006782
wavelet-HH_glszm_LowGrayLevelZoneEmphasis	0.00159
wavelet-HH_glszm_SmallAreaEmphasis	0.003901
wavelet-HH_glszm_SmallAreaLowGrayLevelEmphasis	0.038128
wavelet-LL_glszm_SmallAreaLowGrayLevelEmphasis	-0.01804

Table S10. Radiomics features identified in the analysis of the YOLOv3 dataset and their lambda score.

Feature name	Lambda
original_gldm_HighGrayLevelEmphasis	-0.0307695
original_glrlm_LongRunHighGrayLevelEmphasis	-0.00035511
original_glrlm_ShortRunLowGrayLevelEmphasis	-0.0922137
original_glszm_LargeAreaLowGrayLevelEmphasis	0.0107439
original_glszm_SmallAreaEmphasis	0.0265081
exponential_firstorder_Kurtosis	0.00206107
exponential_firstorder_Median	-0.0502144
exponential_glcm_Idmn	0.0172652
exponential_glcm_JointEnergy	0.0355724
exponential_gldm_LargeDependenceHighGrayLevelEmphasis	-0.0115515
exponential_glszm_GrayLevelVariance	0.120248
exponential_ngtdm_Coarseness	-0.0320669
gradient_glcm_Correlation	-0.0251904
gradient_glrlm_RunLengthNonUniformityNormalized	0.136493
lbp-2D_firstorder_10Percentile	-0.054692
lbp-2D_firstorder_90Percentile	-0.0211308
lbp-2D_firstorder_RobustMeanAbsoluteDeviation	-0.00169874
lbp-2D_glrlm_RunEntropy	0.0799155
logarithm_glcm_Correlation	0.00244712
logarithm_glrlm_ShortRunLowGrayLevelEmphasis	-0.0416502
logarithm_glszm_LowGrayLevelZoneEmphasis	-0.0295585
logarithm_glszm_SizeZoneNonUniformity	0.0178617
square_glszm_LowGrayLevelZoneEmphasis	0.0420735
squareroot_firstorder_Kurtosis	0.0409406
squareroot_glszm_HighGrayLevelZoneEmphasis	-0.0399423
squareroot_glszm_SmallAreaLowGrayLevelEmphasis	0.022961
squareroot_ngtdm_Busyness	0.00390109
wavelet-LH_firstorder_Kurtosis	-0.0265017
wavelet-LH_gldm_DependenceVariance	-0.0843548
wavelet-LH_gldm_SmallDependenceEmphasis	-0.0927388
wavelet-LH_glszm_SmallAreaLowGrayLevelEmphasis	-0.0680015
wavelet-LH_glszm_ZoneEntropy	0.0303013
wavelet-LH_ngtdm_Contrast	0.0800897
wavelet-HL_firstorder_Mean	0.000534665
wavelet-HL_firstorder_Median	0.0620706
wavelet-HL_firstorder_Skewness	0.0139484
wavelet-HL_gldm_DependenceEntropy	0.0255289
wavelet-HL_glrlm_LongRunLowGrayLevelEmphasis	-0.0709579
wavelet-HL_glrlm_ShortRunEmphasis	0.125298
wavelet-HL_glszm_LargeAreaLowGrayLevelEmphasis	0.00545148
wavelet-HL_glszm_LowGrayLevelZoneEmphasis	-0.0263626
wavelet-HH_firstorder_Median	0.0439149

wavelet-HH_firstorder_Skewness	0.0837893
wavelet-HH_glcm_Imc2	-0.206597
wavelet-HH_glrlm_RunLengthNonUniformityNormalized	-0.0275014
wavelet-HH_glrlm_ShortRunEmphasis	-0.0268027
wavelet-HH_glszm_LargeAreaHighGrayLevelEmphasis	-0.088222
wavelet-HH_glszm_SizeZoneNonUniformityNormalized	0.0776143
wavelet-LL_glszm_GrayLevelVariance	0.0112277
wavelet-LL_glszm_SmallAreaLowGrayLevelEmphasis	-0.0282413
wavelet-LL_ngtdm_Busyness	0.0591829

Table S11. Radiomics features identified in the analysis of the Viola-Jones dataset and their lambda score.

Feature name	Lambda
original_glrlm_LongRunHighGrayLevelEmphasis	-0.02305
original_glszm_LargeAreaLowGrayLevelEmphasis	0.022992
original_glszm_LowGrayLevelZoneEmphasis	0.044806
exponential_glcm_ClusterShade	0.023199
exponential_glrlm_LongRunLowGrayLevelEmphasis	0.011298
exponential_glrlm_RunLengthNonUniformityNormalized	0.010645
exponential_glrlm_RunVariance	0.022613
exponential_glrlm_ShortRunLowGrayLevelEmphasis	-0.01934
exponential_glszm_ZonePercentage	0.017238
exponential_glszm_ZoneVariance	0.002615
exponential_ngtdm_Strength	0.023735
gradient_firstorder_10Percentile	0.005552
gradient_firstorder_Kurtosis	0.047964
gradient_firstorder_Minimum	0.010106
gradient_glrlm_RunLengthNonUniformityNormalized	0.152847
gradient_glszm_LargeAreaEmphasis	-0.01393
gradient_glszm_SmallAreaEmphasis	-0.04935
logarithm_firstorder_Kurtosis	0.025563
logarithm_firstorder_Skewness	-0.00622
logarithm_glszm_SmallAreaLowGrayLevelEmphasis	-0.05485
logarithm_ngtdm_Strength	-0.02842
square_ngtdm_Coarseness	0.004001
squareroot_glcm_ClusterShade	-0.01944
squareroot_glrlm_ShortRunLowGrayLevelEmphasis	-0.01013
squareroot_glszm_LowGrayLevelZoneEmphasis	0.023115
squareroot_ngtdm_Contrast	-0.02298
squareroot_ngtdm_Strength	-0.05153
wavelet-LH_firstorder_Skewness	0.026742
wavelet-LH_glcm_ClusterProminence	-0.05829
wavelet-LH_glcm_Idmn	-0.00129
wavelet-LH_glcm_Imc1	0.02695
wavelet-LH_glszm_SmallAreaEmphasis	-0.02663
wavelet-HL_firstorder_Skewness	-0.05648
wavelet-HL_gldm_DependenceNonUniformityNormalized	-0.03142
wavelet-HL_glszm_LargeAreaHighGrayLevelEmphasis	0.010999
wavelet-HH_firstorder_Skewness	0.006642
wavelet-HH_glcm_ClusterShade	0.003819
wavelet-HH_glcm_Imc2	-0.03124
wavelet-HH_gldm_DependenceNonUniformityNormalized	-0.03556
wavelet-HH_glszm_SizeZoneNonUniformityNormalized	0.065
wavelet-HH_glszm_SmallAreaLowGrayLevelEmphasis	0.01799

Table S12. The precision metrics of 3 best breast lesion classification models trained with the 5-fold-cross-validation and 10-fold-cross-validation and 30%, 25%, and 20% holdout on training set of Manual Segmentation, YOLOv3, and Viola-Jones datasets Classification Subsets. The selected algorithms were evaluated with respect to their AUROC, accuracy, sensitivity, and specificity. The metrics for the outstanding classification model obtained for Manual Segmentation, YOLOv3, and Viola-Jones dataset were underlined and bolded.

Dataset	Training	Algorithm	AUROC	Accuracy(%)	Sensitivity(%)	Specificity(%)
Manual Segmentation	5-fold-cross-validation	Linear SVM	0.89	83.33	80.56	87.50
		Weighted KNN	**0.94**	**85.00**	**83.33**	**87.50**
		Ensemble Subspace Discriminant	0.91	83.33	86.11	79.17
	10-fold-cross-validation	Linear SVM	0.89	83.33	80.56	87.50
		Weighted KNN	**0.94**	**85.00**	**83.33**	**87.50**
		Ensemble Subspace Discriminant	0.91	81.67	83.33	79.17
	30% holdout validation	Linear SVM	0.89	83.33	80.56	87.50
		Weighted KNN	**0.94**	**85.00**	**83.33**	**87.50**
		Ensemble Subspace Discriminant	0.90	81.67	83.33	79.17
	25% holdout validation	Cubic SVM	0.91	85.00	83.33	87.50
		Fine KNN	0.82	81.67	80.56	83.33
		Ensemble Subspace Discriminant	0.92	83.33	83.33	83.33
	20% holdout validation	Linear SVM	0.89	83.33	80.56	87.50
		Weighted KNN	0.91	85.00	83.33	87.50
		Ensemble Subspace Discriminant	0.91	81.67	83.33	79.17
YOLOv3	5-fold-cross-validation	Linear SVM	0.74	66.67	63.89	70.83
		Ensemble Subspace KNN	**0.81**	**70.00**	**70.00**	**70.83**
		Ensemble Bagged Trees	0.77	66.67	66.67	66.67
	10-fold-cross-validation	Linear SVM	0.74	66.67	63.89	70.83
		Ensemble Subspace KNN	0.81	71.67	75.00	66.67
		Ensemble Bagged Trees	0.77	71.67	72.22	70.83
	30% holdout validation	Coarse Gaussian SVM	0.73	73.33	83.33	58.33
		Fine KNN	0.73	73.33	75.00	70.83

		Ensemble Subspace Discriminant	0.72	63.33	63.89	62.50
		Quadratic SVM	0.79	40.00	00.00	100.0
	25% holdout validation	Ensemble Bagged Trees	0.79	71.67	80.56	58.33
		Ensemble Subspace Discriminant	0.74	66.67	66.67	66.67
	20% holdout validation	Ensemble Bagged Trees	0.78	71.67	75.00	66.67
		Linear SVM	0.74	66.67	63.89	70.83
		Weighted KNN	0.75	66.67	58.33	79.17
		Cosine KNN	0.67	55.00	52.78	58.33
	5-fold-cross-validation	**Median KNN**	**0.70**	**61.67**	**61.11**	**62.50**
		Ensemble Subspace Discriminant	0.66	60.00	69.44	45.83
		Cosine KNN	0.67	55.00	52.78	58.33
	10-fold-cross-validation	Linear SVM	0.33	40.00	00.00	100.00
		Ensemble Subspace Discriminant	0.66	58.33	66.67	45.83
	30% holdout validation	Coarse Gaussian SVM	0.65	68.33	86.11	41.67
Viola-Jones		Fine Tree	0.59	61.67	61.11	62.50
		Linear SVM	0.33	40.00	00.00	100.00
	25% holdout validation	GaussianNaïve Bayes	0.59	41.67	11.11	87.50
		Kernel Naïve Bayes	0.59	48.33	44.44	54.17
		Linear SVM	0.33	40.00	00.00	100.00
		Linear SVM	0.33	40.00	00.00	100.00
	20% holdout validation	Kernel Naïve Bayes	0.59	48.33	44.44	54.17
		Median KNN	0.70	61.67	61.11	62.50

Figure S1. Augmentation scenarios: Image pre-processing. (A) Original image; (B) Image decomposed with UDWT (HH); (C) Image decomposed with UDWT (HL); (D) Image decomposed with UDWT (LH); (E) Image decomposed with UDWT (LL); (F) Exponential derivative of the original image; (G) Logarithmic derivative of the original image; (H) Laplacian of Gaussian of the original image; (I) Squared derivative of the original image; (J) Square root derivative of the original image.

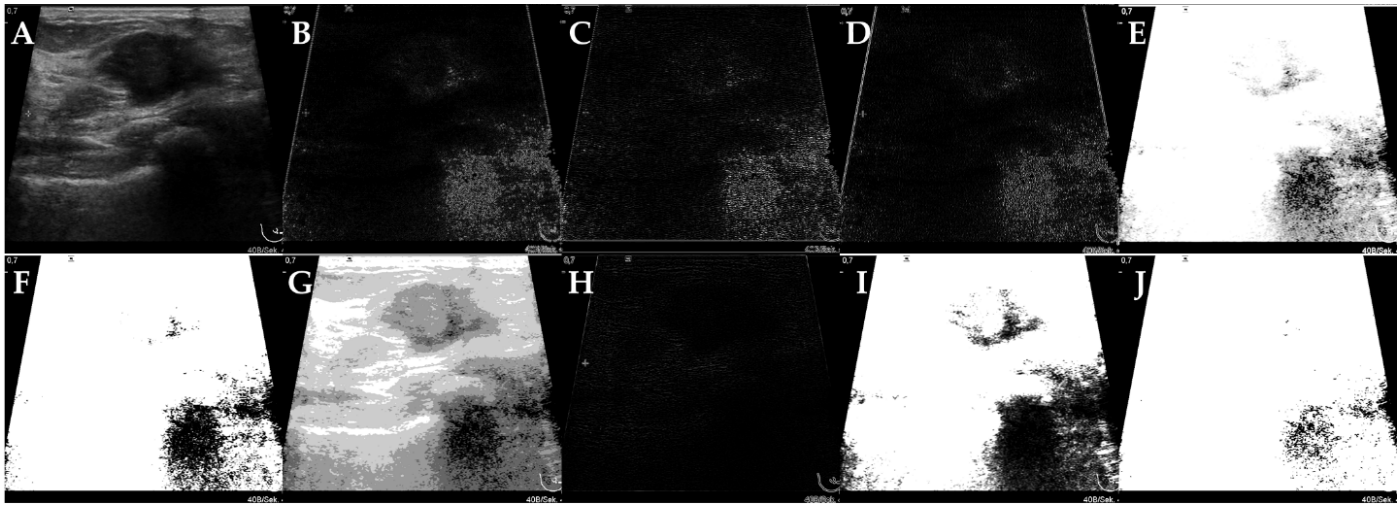

Figure S2. Augmentation scenarios: Rotations. Original image rotated: (A-i) Clockwise by 45º; (A-ii) Clockwise by 90º; (A-iii) Clockwise by 135º; (B-i) Counterclockwise by 45º; (B-ii) Counterclockwise by 90º; (B-iii) Counterclockwise by 135º.

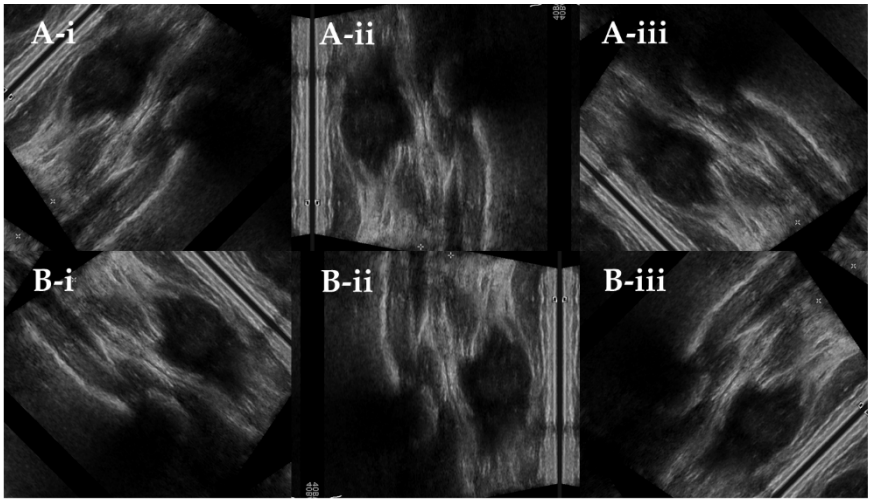

Figure S3. Augmentation scenarios: Translation. Original image translated: (i) Right (x-axis) and Down (y-axis); (ii) Right (x-axis) and Up (y-axis); (iii) Left (x-axis) and Down (y-axis); (iv) Left (x-axis) and Up (y-axis).

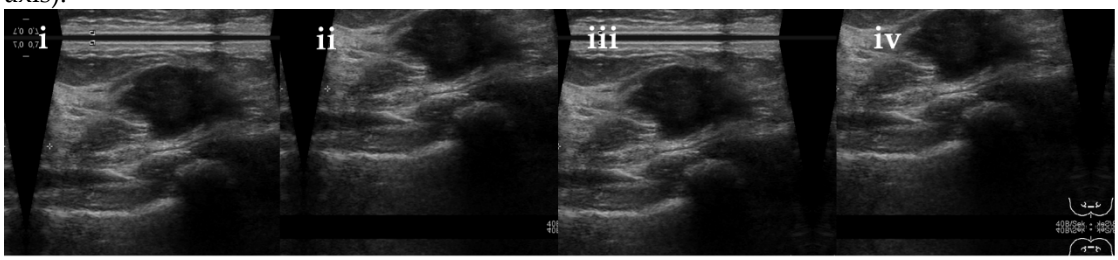

Figure S4. Augmentation scenarios: Flips. Original image flipped about: (A-i) Its origin; (A-ii) X-axis; (A-iii) Y-axis.

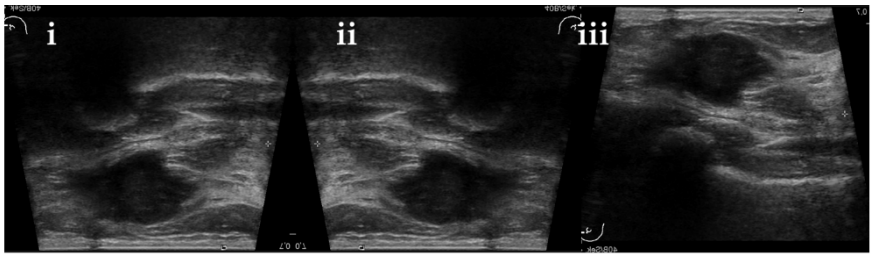

Figure S5. Augmentation scenarios: Shearing with respect to y-axis. Original image sheared right by: (A-i) 5º; (A-ii) 10º; (A-iii) 15º; (A-iv) 20º, (A-v) 25º; (A-vi) 30º. Original image flipped about its origin and sheared right by: (B-i) 5º; (B-ii) 10º; (B-iii) 15º; (B-iv) 20º, (B-v) 25º; (B-vi) 30º. Original image flipped about x-axis and sheared right by: (C-i) 5º; (C-ii) 10º; (C-iii) 15º; (C-iv) 20º, (C-v) 25º; (C-vi) 30º. Original image flipped about y-axis and sheared right by: (D-i) 5º; (D-ii) 10º; (D-iii) 15º; (D-iv) 20º, (D-v) 25º; (D-vi) 30º. Original image sheared left by: (E-i) 5º; (E-ii) 10º; (E-iii) 15º; (E-iv) 20º, (E-v) 25º; (E-vi) 30º. Original image flipped about its origin and sheared left by: (F-i) 5º; (F-ii) 10º; (F-iii) 15º; (F-iv) 20º, (F-v) 25º; (F-vi) 30º. Original image flipped about x-axis and sheared left by: (G-i) 5º; (G-ii) 10º; (G-iii) 15º; (G-iv) 20º, (G-v) 25º; (G-vi) 30º. Original image flipped about y-axis and sheared left by: (H-i) 5º; (H-ii) 10º; (H-iii) 15º; (H-iv) 20º, (H-v) 25º; (H-vi) 30º.

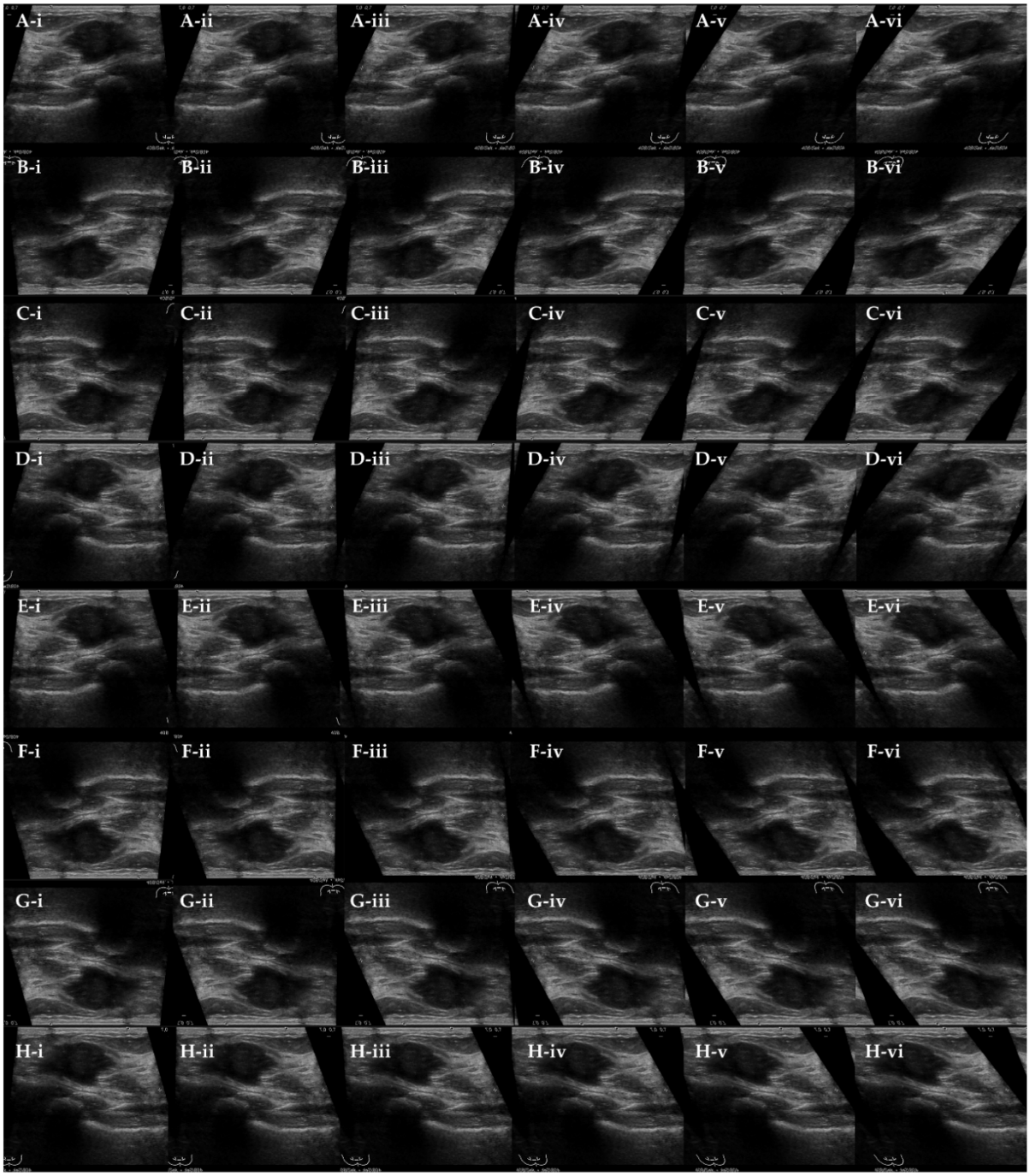

Figure S6. Augmentation scenarios: Shearing with respect to x-axis. Original image sheared down by: (A-i) 5º; (A-ii) 10º; (A-iii) 15º; (A-iv) 20º, (A-v) 25º; (A-vi) 30º. Original image flipped about its origin and sheared down by: (B-i) 5º; (B-ii) 10º; (B-iii) 15º; (B-iv) 20º, (B-v) 25º; (B-vi) 30º. Original image flipped about x-axis and sheared down by: (C-i) 5º; (C-ii) 10º; (C-iii) 15º; (C-iv) 20º, (C-v) 25º; (C-vi) 30º. Original image flipped about y-axis and sheared down by: (D-i) 5º; (D-ii) 10º; (D-iii) 15º; (D-iv) 20º, (D-v) 25º; (D-vi) 30º. Original image sheared up by: (E-i) 5º; (E-ii) 10º; (E-iii) 15º; (E-iv) 20º, (E-v) 25º; (E-vi) 30º. Original image flipped about its origin and sheared up by: (F-i) 5º; (F-ii) 10º; (F-iii) 15º; (F-iv) 20º, (F-v) 25º; (F-vi) 30º. Original image flipped about x-axis and sheared up by: (G-i) 5º; (G-ii) 10º; (G-iii) 15º; (G-iv) 20º, (G-v) 25º; Original image flipped about y-axis and sheared up by: (H-i) 5º; (H-ii) 10º; (H-iii) 15º; (H-iv) 20º, (H-v) 25º; (H-vi) 30º.

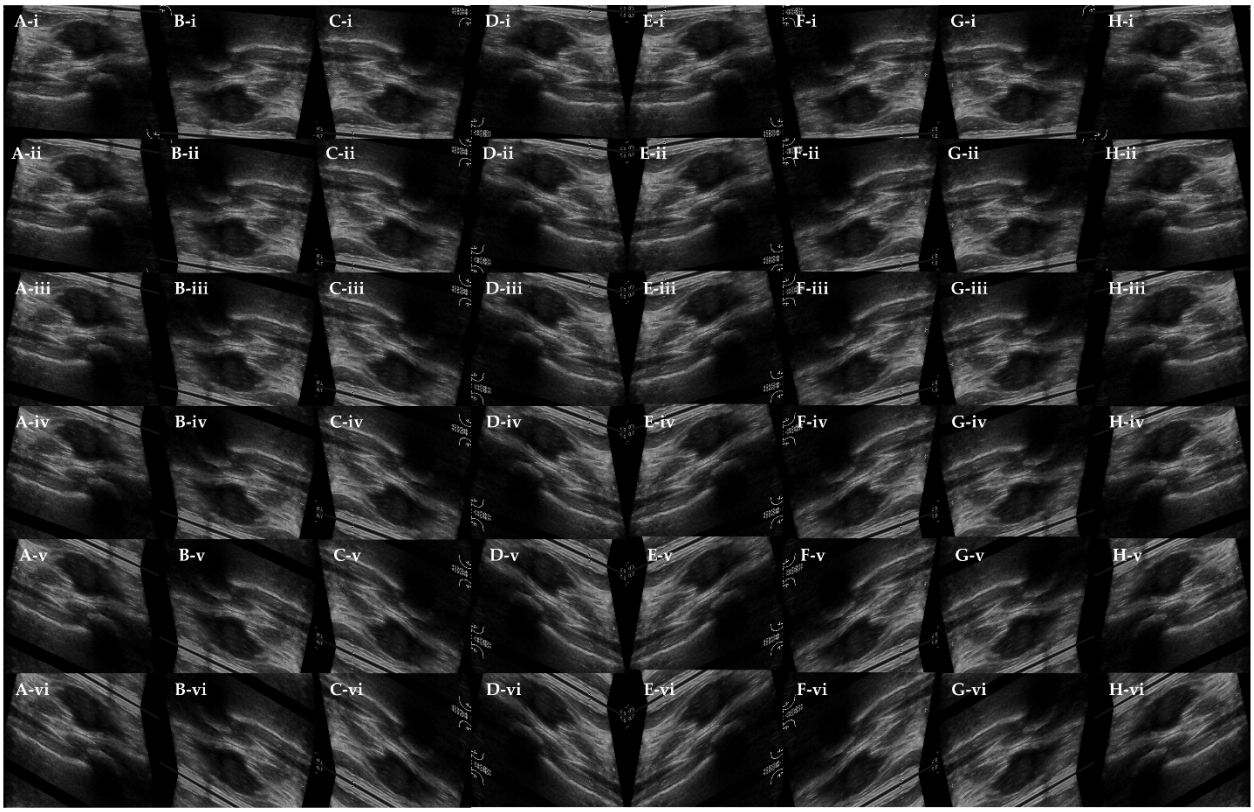

Figure S7. Labeling of positive and negative image samples for training Viola-Jones detection classifiers.

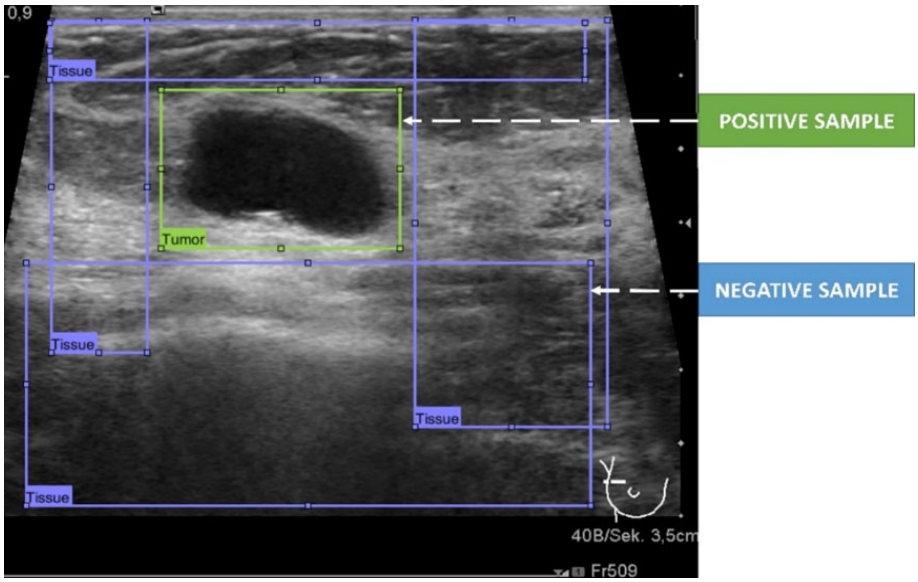

Figure S8. Recall-IoU and recall-LE characteristics resulting from the evaluation of the best breast lesion detection algorithm on the validation set. (A-i) YOLOv3 detection functions trained with transfer leraining by 'fine tuning' scored with different IoU thresholds; (A-ii) YOLOv3 detection functions trained with transfer leraining by 'fine tuning' scored with different LE thresholds; (B-i) YOLOv3 detection functions trained with transfer leraining by 'fine tuning' scored with different IoU thresholds; (B-ii) YOLOv3 detection functions trained with transfer leraining by 'fine tuning' scored with different LE thresholds; (C-i) Viola-Jones detection functions scored with different IoU thresholds; (C-ii) Viola-Jones detection functions scored with different LE thresholds.

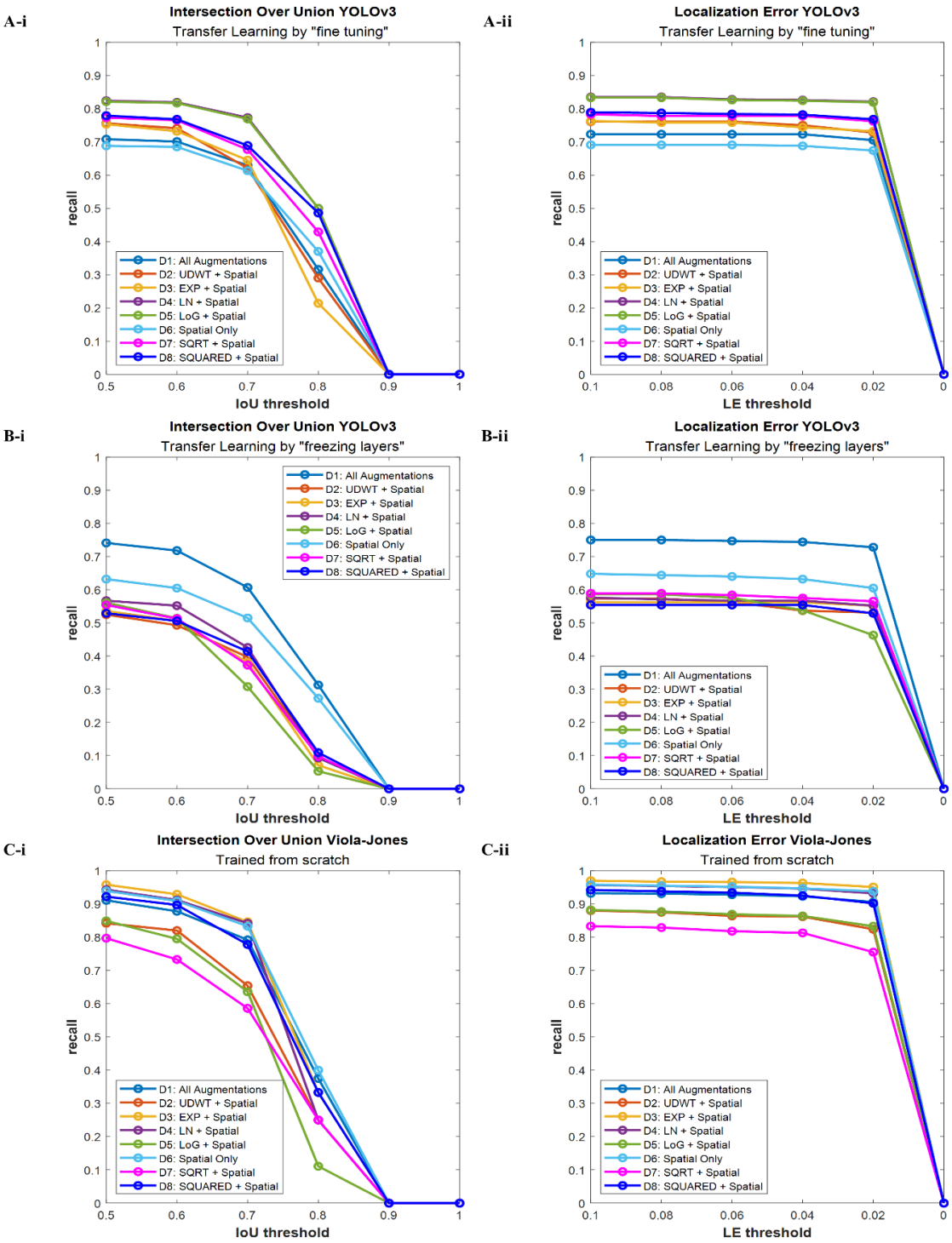

Figure S9. Recall-IoU and recall-LE characteristics resulting from the evaluation of the best breast lesion detection algorithm on the second data pool. (A-i) YOLOv3 detection functions scored with different IoU thresholds; (A-ii) YOLOv3 detection functions scored with different LE thresholds; (B-i) Viola-Jones detection functions scored with different IoU thresholds; (B-ii) Viola-Jones detection functions scored with different LE thresholds.